




Effects of using ammonia as a primary fuel on engine performance and emissions in an ammonia/biodiesel dual-fuel CI engine

Ebrahim Nadimi¹  | Grzegorz Przybyła¹  | David Emberson² |
Terese Løvås² | Łukasz Ziółkowski¹ | Wojciech Adamczyk¹ 

¹Department of Thermal Technology, Faculty of Energy and Environmental Engineering, Silesian University of Technology, Gliwice, Poland

²Department of Energy and Process Engineering, Norwegian University of Science and Technology, NTNU, Trondheim, Norway

Correspondence

Ebrahim Nadimi, Department of Thermal Technology, Faculty of Energy and Environmental Engineering, Silesian University of Technology, Gliwice, Poland.
Email: enadimi@polsl.pl

Funding information

POLNOR, Grant/Award Number: NOR/POLNOR/ACTIVATE/0046/2019-00; AVL List

Summary

Ammonia is a promising alternative fuel that can replace current fossil fuels. Hydrogen carrier, zero carbon base emissions, liquid unlike hydrogen, and can be produced using renewable resources, making ammonia a future green fuel for the internal combustion engine. This study aims to show the procedure of utilizing ammonia as a primary fuel with biodiesel in a dual-fuel mode. Hence, a single-cylinder diesel engine was retrofitted to inject ammonia into the intake manifold, and then a pilot dose of biodiesel is sprayed into the cylinder to initiate combustion of the premixed ammonia-air mixture. The effects of various ammonia mass flow rates with a constant biodiesel dose on engine performance and emissions were investigated. Furthermore, a one-dimensional model has been developed to analyze the combustion of ammonia and biodiesel. The results reveal that 69.4% of the biodiesel input energy can be replaced by ammonia but increasing the ammonia mass flow rate slightly decreases the brake thermal efficiency. Moreover, increasing the ammonia load contribution significantly reduced the emissions of CO_2 , CO , and HC but increased the emission of NO . It was found that ammonia delayed the start of combustion by 2.6CAD compared with pure biodiesel due to the low in-cylinder temperature and the high resistance of ammonia to autoignition. However, the combustion duration of biodiesel/ammonia decreased 19CAD compared with only biodiesel operation at full load, since most of the heat was released during the pre-mixed combustion phase.

Highlights

- Ammonia biodiesel dual-fuel CI engine has been investigated experimentally.
- Maximum 69.4% of the input energy is provided by ammonia in reasonable operation.
- Higher ammonia contribution in the engine load delays the SOC and decreases the combustion duration.

This is an open access article under the terms of the [Creative Commons Attribution](https://creativecommons.org/licenses/by/4.0/) License, which permits use, distribution and reproduction in any medium, provided the original work is properly cited.

© 2022 The Authors. *International Journal of Energy Research* published by John Wiley & Sons Ltd.

- Significant reduction in CO_2 , CO , and HC emissions in the ammonia-/bio-diesel-fueled engine.

KEYWORDS

ammonia, biodiesel, CI engine, dual fuel, emissions

1 | INTRODUCTION

Fossil fuels, greenhouse gases, and their effects on climate change are required to be replaced by renewable energy sources to slow down the emission of carbon dioxide. To combat these worldwide challenges, the legitimately binding international agreement on climate change, the 2015 Paris Agreement provided a global framework for reducing greenhouse gases in the next decades. Hence, the European Union countries have an aim to decrease the emissions of greenhouse gases by 55% by 2030.¹ Therefore, alternative carbon-free fuels, such as ammonia and hydrogen, are a good way to replace fossil fuels and stop the emission of carbon dioxide. However, the big problem with hydrogen is storing in the high pressure at a reasonable cost because of the extremely low density of gaseous hydrogen. Among all green fuels such as ethanol,² methanol,³ and methyl ester,⁴ ammonia (NH_3) is currently attracting a lot of interest as a potential alternative to fossil fuels.⁵⁻⁷ It is a good hydrogen carrier (17.8% by mass), is liquid and easy to store under low pressure, and is also one of the most produced chemicals in the world. Additionally, ammonia already has a great established infrastructure for distribution, production, and handling, as it is used as fertilizer in the agriculture industry. However, the practical usage of liquid ammonia as fuel for internal combustion engine (ICE) requires many technical and operational difficulties to be surmounted. Ammonia has different characteristics from common fossil fuels. High resistance to auto ignition, low flame speed, and corrosivity are challenges of ammonia that make it even harder to apply in ICE.⁸⁻¹⁰ The beginning of using ammonia as fuel goes back to 1943 in Belgium due to a shortage of diesel fuel during World War Two.¹¹ Subsequently, in the 1960s, the possibility of applying ammonia to ICE was examined, providing primary guidance concerning ammonia as a fuel in ICE.¹²⁻¹⁵

In recent years, researchers have been working to overcome the challenges of using ammonia as fuel for both CI and spark ignition (SI) engines. However, a new review paper¹⁶ shows that most research is currently concentrated in SI engines because ammonia is more favorable for use in SI engines. Schönborn¹⁷ by zero-dimensional chemical kinetic calculation estimated the minimum required Compression Ratio (CR) of 27 to ignite pure ammonia in the CI

engine. Grannell et al.¹⁸ investigated mixtures of gasoline and gaseous ammonia in the SI engine in varied ammonia/gasoline ratios, as well as various CR. Their findings revealed that a significant portion of gasoline can be substituted with ammonia. Nevertheless, they suggested a CR of 10:1 for the ammonia gasoline dual-fuel SI engine. Salek et al.¹⁹ numerically studied the impact of adding 10% of ammonia on engine performance and emissions in a wide range of engine speeds for the SI engine using AVL BOOST software. The results show that 10% of ammonia injection reduces the in-cylinder temperature by 50 K, resulting in a significant reduction in NO_x emissions by 50% throughout the different engine speeds. Furthermore, the needed minimum octane number of gasoline for avoiding knock was decreased by the injection of 10% ammonia, indicating that the injection of ammonia could clearly have an effect on engine failure. Nevertheless, it imposed some negative effects on reducing BSFC and increasing HC and CO emissions. Yapicioglu and Dincer²⁰ conducted experimental research on injecting ammonia in SI engine. The primary objective of this study is to utilize ammonia to reduce carbon emissions. Based on their findings, introducing ammonia reduced the gasoline engine's CO_2 emission. In addition, it resulted in a significantly reduction of engine energy and exergy efficiency. The recent paper carried out by Mounaïm-Rousselle et al.²¹ provides new information on operation limits in ammonia-fueled gasoline direct injection (GDI) SI engine, especially to find the lowest possible load limit when the engine is fed with pure ammonia. However, they extended the operating limitations by adding less than 10% of hydrogen to ammonia. Although the ammonia-fueled engine does not produce carbon-based emissions, it can emit high NO_x emissions. However, their results show that adding 10% of H_2 to ammonia significantly decreases NO_x emissions up to 40%. Lhuillier et al.²² experimentally investigated engine performance, emissions, and combustion characteristics of an SI engine fueled with premixed ammonia, hydrogen, and air mixtures. They tested mixtures of gaseous ammonia with different portions of hydrogen as well as various equivalence ratios. Their results illustrate that the higher hydrogen fraction in the stoichiometry mixture decreases the indicated efficiency, but the efficiency increases when the equivalence ratio decreases. Moreover, when the equivalence ratio is raised above stoichiometry, the unburned ammonia rises significantly. Sechul et al.²³

experimentally studied ammonia blended with natural gas in the SI engine. According to their findings, CO_2 emissions were reduced by almost 28% when natural gas was replaced with ammonia for more than 50% of the volume portion. However, considering combustion efficiency and emissions, the air/fuel ratio reached a high limit around λ 1.5. As mentioned above, using only ammonia in CI engines requires high CR; hence, ammonia can be utilized as a secondary fuel with a small dose of diesel or biodiesel to ignite combustion in a dual-fuel mode without considerable modification in the engine.²⁴ Reiter and Kong²⁵ investigated the impacts of injecting gaseous ammonia into the intake manifold on the emissions and combustion characteristics of the CI engine. They tested different ratios of ammonia/diesel to obtain constant power in the operating range of 40% to 60% of the input energy provided by ammonia to achieve the optimal fuel efficiency. Their experimental results show that when the ammonia energy contributes to more than 60% of the total energy, the NO emissions rise significantly, but soot emissions decreased for a higher ammonia ratio. Their other similar work²⁶ proved that engine operation was successful for 95% of energy supplied by ammonia; however, the unburned NH_3 was significantly higher due to unsuccessful combustion. Nevertheless, reasonable efficiency can be achieved if 80% of the total energy is supplied by ammonia.

A novel combustion strategy for using ammonia in CI engine has been suggested by Lee and Song²⁷ to reduce NO emissions. Parametric research has been performed to validate and evaluate the characteristics of the ammonia-fueled engine by applying the suggested combustion strategy. They discussed engine operation characteristics according to the ammonia dose, start of injection (SOI) timing, and NO emissions. Their findings indicate that for constant amount of ammonia and diesel fuel, NO production is a strong function of SOI instead of the load of the engine. Hence, NO emission was reduced from 8500 ppm to 3040 ppm by changing the SOI timing. Recently, Yousefi et al.²⁸ investigated the impacts of the ammonia energy fraction with diesel injection timing on engine performance and emissions. Their results reveal that the NO_x emissions decreased by 58.8% when the ammonia energy percentage was increased from 0 to 40%. However, it increased the N_2O emission, which has a higher greenhouse effect.

In recent years, there has been renewed enthusiasm for utilizing ammonia as a primary fuel for ICE. Nevertheless, it is evident from the above literature review that there is a significant research gap in ammonia-/biodiesel-fueled CI engine. Comprehensive research has to be done to effectively utilize ammonia while reducing emissions in the diesel engine. Therefore, in this paper, a strategy of using ammonia with biodiesel as a secondary fuel is proposed to operate with the lowest possible biodiesel and high amount of ammonia in different loads with reasonable operation. For the first

time, ammonia with biodiesel dual-fuel CI engine has been studied. Hence, the effects of various ammonia mass flows with two constant pilot doses of biodiesel on combustion, emissions, and engine performance are investigated and compared with pure biodiesel operation. Additionally, a 1D model is built and developed to analyze ammonia with biodiesel combustion characteristics.

2 | TEST RIG AND EXPERIMENTAL SETUP

2.1 | Test rig

The tests were performed on a single-cylinder 4-stroke Lifan diesel engine C186F with forced air cooling system. The engine's main specifications are listed in Table 1. The engine has been retrofitted to operate with port injection of ammonia and then will be installed in the tractor for use in the agricultural sector. Gaseous ammonia at 2 bar was injected into the port near the inlet valve, through the pipe inserted into the intake manifold, and the mass flow of ammonia was measured using a Coriolis flow meter. A surge tank has been installed in the intake manifold to measure the constant air mass flow rate, and also to avoid the backflow of ammonia from the intake manifold to the environment. The temperature of the port, exhaust gas, and ambient as well as the air and ammonia mass flow rate were monitored by LabVIEW software and National Instruments hardware. The engine has been coupled by the vibration damping shaft to the

TABLE 1 Engine main specifications

Engine information	Valves	Units
Engine type	4 stroke, CI	
Number of cylinders	1	
Bore \times Stroke	86 \times 70	mm \times mm
Compression ratio	16.5:1	
Maximum power (3500 rpm)	6.4	kW
Piston shape	ω bowl	
IVO	14	BTDC
IVC	45	ABDC
EVO	50	BBDC
EVC	16	ATDC
SOI	15.5	BTDC
Injection pressure	200	bar
Intake temperature	10	$^{\circ}C$
Intake pressure	93.19	kPa
Engine speed	1500	rpm

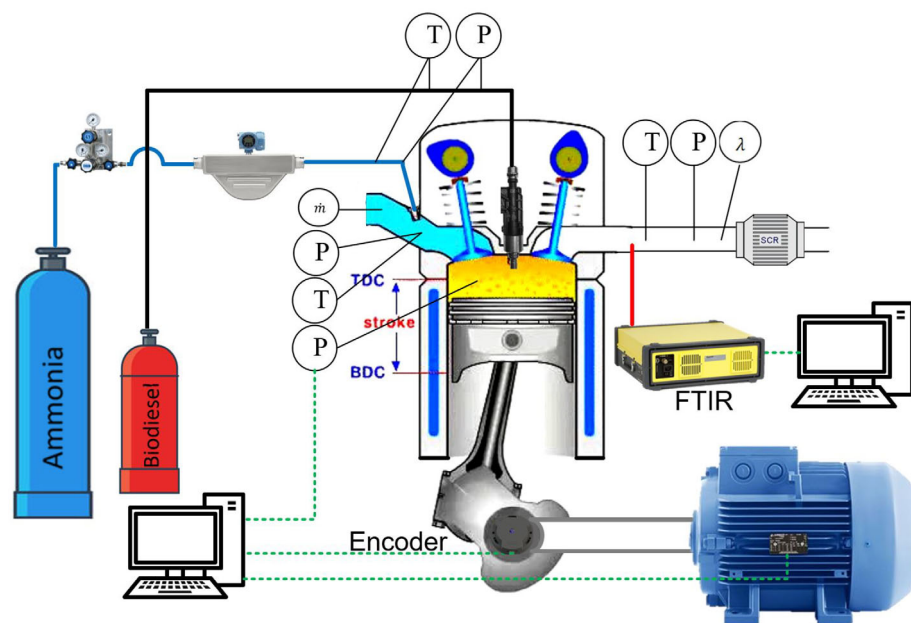


FIGURE 1 Schematic of the experiment for the ammonia/biodiesel dual-fuel engine. P and T represent the measurement points of pressure and temperature, respectively

electric motor to adjust the engine load and speed for the test. The in-cylinder pressure was measured with a resolution of 1024 measuring points per one shaft revolution and for 100 consecutive cycles using a piezoelectric pressure transducer. An encoder with 0.35 CA resolution was installed on the engine shaft to sample the electrical signal from the pressure transducer to identify the piston position at TDC. A sample of the exhaust gas was analyzed using Fourier transform infrared spectroscopy (FTIR), gas analyzer, and particulate matter (PM). The FTIR is a Gasetm DX4000 gas analyzer, which is operated by Calcmnet software. The Calcmnet can simultaneously analyze 50 gas components in wet and corrosive gas streams, and it has various spectrum libraries in different ranges to determine the concentration of each species. However, the ammonia concentration was beyond the measurement ranges, so it is not available. The FTIR has an accuracy of less than 2%. Furthermore, the PM measurement device has a precision of less than $\pm 3\%$ and measures particle sizes from 0.04 to 10 μm with particle mass concentrations up to 250 mg/m^3 under normal conditions and dry exhaust gas. Each parameter was measured every second for 5 min in the steady-state running engine for each operating point.

2.2 | Experiment procedure

Figure 1 illustrates the schematic of the test. In this figure, P and T show the measuring points for pressure and temperature. In all tests, the rotational speed has been fixed at 1500 rpm. The engine has been operated with biodiesel at different loads to determine the baseline. The approach

for ammonia port injection is defined in this way that the engine is operated with biodiesel in low load and with constant biodiesel mass flow rate, and then ammonia is injected to increase torque and power. Hence, Table 2 presents the procedure of the two sets of ammonia and biodiesel tests. In the first test, biodiesel load contribution (BLC) was 10%, ie, the engine has been operated with biodiesel and the measured load and biodiesel mass flow rate were 10% and $\dot{m}_{bio} = 0.107\text{g}/\text{s}$, respectively. Then, the ammonia mass flow is increased to obtain higher loads at the same operating point as the biodiesel baseline. The second test is similar to the test one, but with this difference that the engine was run with biodiesel at a low load of 3.5% with constant $\dot{m}_{bio} = 0.082\text{g}/\text{s}$. By increasing the ammonia mass flow, ammonia load contribution (ALC), and ammonia energy contribution (AEC), which is defined in Equation (1), have been increased since the biodiesel mass flow rate and the BLC were constant in the two sets of tests. The maximum input AEC is 59.1% and 69.4% at full load for test one with $\dot{m}_{bio} = 0.107\text{g}/\text{s}$, and test two with $\dot{m}_{bio} = 0.082\text{g}/\text{s}$, respectively. However, reducing the biodiesel mass flow lower than $\dot{m}_{bio} = 0.082\text{g}/\text{s}$ to replace it with more ammonia to obtain higher input AEC causes a significant amount of ammonia slip. The exhaust gas sample is interred to FTIR, gas analyzer, and PM measurement before SCR.

2.3 | One-dimensional model and data analysis

One-dimensional (1D) model of ammonia/biodiesel dual-fuel engine was built and developed using the AVL

TABLE 2 Ammonia/biodiesel tests conditions

NO.	BLC	ALC	Load	\dot{m}_{bio}	\dot{m}_{NH_3}	w_{NH_3}	\dot{m}_{air}	AEC	
Unit	%	%	%	g/s	g/s	kg/kg	g/s	%	
Set 1	1	10.0	10.0	20	0.107	0.045	0.29	6.47	17.1
	2	10.0	25.3	35	0.107	0.100	0.48	6.25	32.2
	3	10.0	37.1	47	0.107	0.141	0.56	6.16	40.0
	4	10.0	48.8	59	0.107	0.186	0.63	5.97	46.6
	5	10.0	60.6	71	0.107	0.227	0.67	5.83	51.0
	6	10.0	78.2	88	0.107	0.293	0.73	5.63	57.2
	7	10.0	90.0	100	0.107	0.327	0.75	5.44	59.1
Set 2	8	3.5	16.5	20	0.082	0.107	0.56	6.36	40.0
	9	3.5	31.8	35	0.082	0.157	0.65	6.13	49.2
	10	3.5	43.6	47	0.082	0.213	0.72	6.02	55.6
	11	3.5	55.3	59	0.082	0.260	0.76	5.94	60.7
	12	3.5	67.1	71	0.082	0.293	0.78	5.69	65.0
	13	3.5	84.7	88	0.082	0.361	0.81	5.47	67.1
	14	3.5	96.5	100	0.082	0.398	0.82	5.27	69.4

TABLE 3 Biodiesel properties

Property	Value	Unit
Name	Bioester	–
<i>C</i>	75.33	kg/kg
<i>H</i>	13.97	kg/kg
<i>O</i>	10.7	kg/kg
Molecular weight	200	kg/kmol
LHV	37.4	MJ/kg
Cetane number	51.0	–
Density	860	kg/m ³
Cold point	–3	°C
Flash point	101	°C
Stoichiometric air/fuel ratio	12.96	–

BOOST software. In addition, the AVL Burn utility was used for post-processing of the measured data, analyzing the pressure profile, and calculating the net heat release rate (HRR). The HRR has been determined from the measured pressure trace through the inverse procedure. Additionally, the combustion timing indicators have been calculated by mass fraction burned (MFB). Hence, the MFB diagram, combustion duration (CD), start of combustion (SOC), and the location of MFB 10%, 50%, 90% (CA10, CA50, and CA90) have been calculated using AVL software. In this study, the SOC refers to the location of the rising point on the MFB curve in the Vibe function.²⁹

Biodiesel fuel (Bioester B100) was provided by Orlen Poludnie company in Poland. The LHV of biodiesel was measured at 37.400 MJ/kg; however, the ammonia LHV is 18.6 MJ/kg.³⁰ The elementary analysis and properties

of biodiesel are listed in Table 3. In this work, the AEC is defined as the ratio of the ammonia input energy to the total input energy in the dual-fuel model in Equation (1).

$$AEC = \frac{\dot{m}_{NH_3} \times LHV_{NH_3}}{\dot{m}_{bio} LHV_{bio} + \dot{m}_{NH_3} LHV_{NH_3}} \quad (1)$$

The friction power of the electric motor at 1500 rpm has been measured, and it is about 0.52 kW. The torque and power are calculated after subtracting the friction power. Therefore, the brake thermal efficiency (BTE) of the engine is defined as follows:

$$BTE = \frac{P_b}{\dot{m}_{bio} \times LHV_{bio} + \dot{m}_{NH_3} \times LHV_{NH_3}} \quad (2)$$

The concentrations of each species were measured during 5 min of steady-state operation in molecules per million in ppm unit and then recalculated according to Equation (3) in 5% of O₂ since the concentration of each species varies for different loads.³¹ Additionally, the brake-specific emission in g/kW.h units is calculated.

$$(X_i)_{5\%O_2} = (X_i)_m \left[\frac{20.9\% - 5\%}{20.9\% - (O_2)_m} \right] \quad (3)$$

Where $(X_i)_m$ and $(O_2)_m$ are the measured concentration of each species and the measured concentration of O₂, respectively.

The equivalent brake-specific fuel consumption is defined in Equation (4) in dual-fuel engine.³²

$$BSFC = \frac{\dot{m}_{bio} + \dot{m}_{NH_3} \frac{LHV_{NH_3}}{LHV_{bio}}}{P_b} \quad (4)$$

Measurement uncertainty has been evaluated through statistical analysis. The SD of the emissions and data obtained from the test rig were calculated using the Equation (5)^{33,34}:

$$SD = \sqrt{\frac{\sum_{i=1}^n (X_i - \bar{X})^2}{(n-1)}} \quad (5)$$

where X_i , and \bar{X} are the measured and mean values, respectively, and n is the number of measurements.

Therefore, uncertainty (U) is defined by^{33,34}:

$$U = \frac{SD}{\sqrt{n}} \quad (6)$$

Furthermore, the coefficient of variation (COV) of 100 continuous cycles for IMEP, P_{max} , and α_{max} was obtained. Therefore, $COV_{P_{max}}$ and $COV_{\alpha_{max}}$ were less than 1% for all tests. However, COV_{IMEP} was less than 2% and 4% for biodiesel and ammonia/biodiesel operations, respectively.

3 | RESULTS

3.1 | Effects of ammonia on engine performance

As mentioned above, the ammonia injection strategy was carried out in such a way that the engine is operated first with only biodiesel at $\dot{m}_{bio} = 0.107\text{g/s}$ in 10% load and secondly at $\dot{m}_{bio} = 0.082\text{g/s}$ in 3.5% load. Hereafter, the ammonia mass flow is increased to obtain the same loads as biodiesel. The maximum power ($P_{b_{max}}$) of the engine at 100% of the load is 3.190 kW, of which 2.356 and 2.576 kW of $P_{b_{max}}$ are provided by ammonia for the tests set 1 and set 2, respectively. The mass flow of ammonia was increased to obtain the same power as only biodiesel tests; however, the brake efficiency of the dual-fuel mode is slightly lower compared with the baseline, as shown in Figure 2. The BTE increases with increasing load and reaches 32.27% at load 88% after that decreased to 31.89% at full load for the biodiesel test. This decline in BTE at full load is due to the high amount of unburned hydrocarbons such as HC , CO , and soot together with high exhaust gas temperature (Figure 3). However, ammonia by decreasing the emission of unburned hydrocarbons

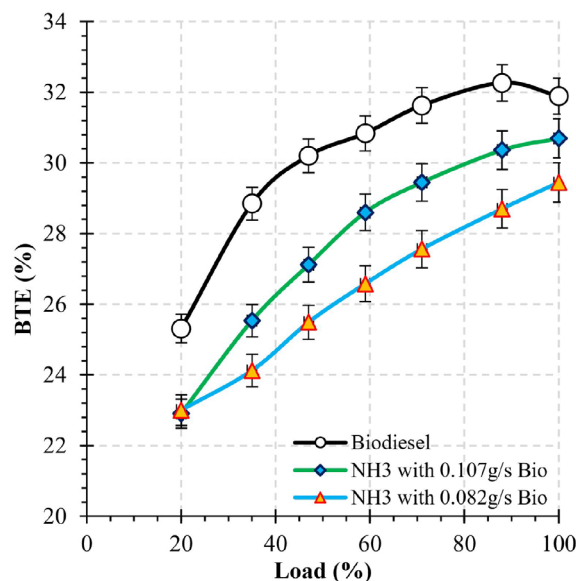


FIGURE 2 Brake thermal efficiency of the ammonia-/biodiesel-fueled engine compared along with biodiesel

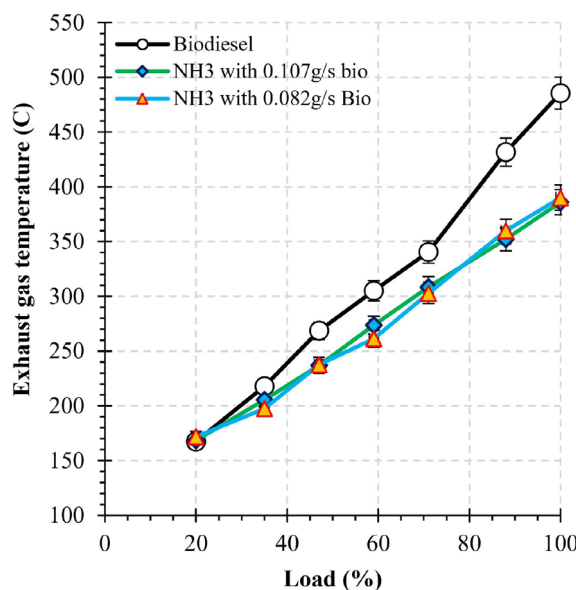


FIGURE 3 Effects of ammonia on exhaust gas temperature compared with biodiesel

obtains a BTE of 30.69% at full load in set 1 test. Moreover, the increase in BTE at higher loads is due to a decrease in the ratio between friction losses and the engine indicated work, resulting in a decrease in the friction power contribution to brake power. Figure 2 also shows that by reducing the biodiesel mass flow rate from $\dot{m}_{bio} = 0.107\text{g/s}$ to $\dot{m}_{bio} = 0.082\text{g/s}$ to obtain a higher ALC, decreases the BTE due to unsuccessful combustion of ammonia with biodiesel, causing a high amount of unburned NH_3 .

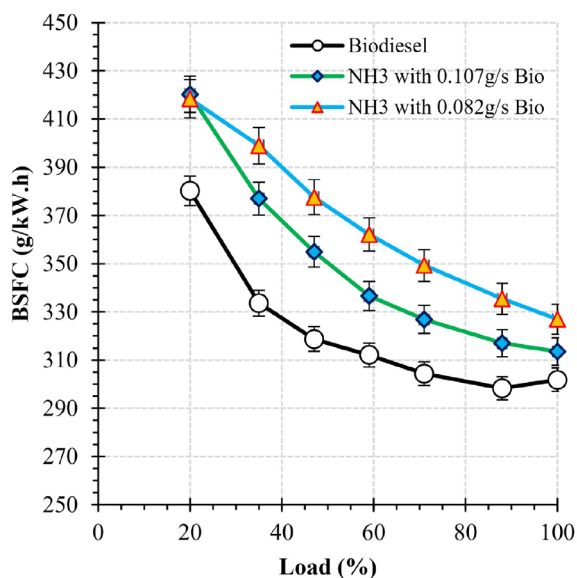


FIGURE 4 Brake-specific fuel consumption of the ammonia/biodiesel with the biodiesel tests corresponds to the engine load

As can be observed in Figure 3, the exhaust gas temperature of the biodiesel test is higher compared with the dual ammonia/biodiesel tests. For example, EGT is reduced by 100 from 485 K for biodiesel to 385 K for ammonia/biodiesel tests at full load due to the lower in-cylinder temperature during the combustion stroke since the in-cylinder temperature of ammonia-/biodiesel-fueled engine is lower than the biodiesel.³⁵ Moreover, the CD of ammonia/biodiesel combustion is lower than that of biodiesel at higher loads, which will be discussed in the next section. Therefore, less heat is released during the expansion stroke, resulting in a temperature drop in the working medium and ultimately a lower exhaust temperature in ammonia/biodiesel operation compared with pure biodiesel, as can be observed in Figure 3. The SCR is activated around 300°C,³⁶ therefore it is only active in higher loads.

Figure 4 illustrates the equivalent BSFC for ammonia/biodiesel tests along with only biodiesel under various loads. The BSFC of ammonia/biodiesel is higher relative to biodiesel operation due to the lower LHV of the ammonia/biodiesel mixture, since LHV_{NH_3} is considerably lower compared with LHV_{bio} (Equation 4). However, the BSFC difference between ammonia-/biodiesel-fueled engine with only biodiesel at 20% of the load is approximately 10.0% due to the ineffective burning of the lean ammonia/air mixture at low loads.³⁷ Nevertheless, this difference will decrease with increasing load. Hence, the BSFC of set 1, set 2, and biodiesel tests are 300.2, 313.5, and 326.8 g/kW.h, respectively.

3.2 | Effects of ammonia on in-cylinder parameters

Figure 5 shows in-cylinder pressure profiles vs load for each operating point. The pressure traces for the biodiesel test on different loads along with the pressure profiles of the full load of set 1 and set 2 are presented in Figure 5A. The location of rapid rise in pressure is constant with increasing load in the pure biodiesel operation, and the pressure curves are also overlapped in the starting of the high pressure. This is due to the fixed start of biodiesel injection at $-15.5CAD$. It was observed that ammonia/biodiesel combustion generally has higher in-cylinder pressure than biodiesel. For example, the peak of the pressure for biodiesel is 76.64 bar and increased to 82.89 bar (8.1% increase) and 87.79 bar (14.5% increase) for set 1 and set 2 at full load, respectively. This is mainly due to ignition delay and the higher premixed ratio compared with biodiesel, as can be seen in the HRR profile in Figure 7A. HRR diagram of the diesel engine normally has four steps, which are ignition delay, premixed combustion, diffusion combustion, and late combustion, sequentially, according to Heywood.³⁸ However, the evaporation phase of the pilot biodiesel in the premixed air-ammonia is very short compared with the only biodiesel operation in which a high amount of ammonia causes one peak in the HRR diagram, and most of the heat is released in premixed combustion. Hence, the location of the peak of the pressure leads to the advance by increasing the ALC, as can be seen in Figure 5B,C. Furthermore, the pressure rise rate profiles are presented in Figure 6 for 20% and 100% loads. The peak of PRR is 5.4 bar/deg at full loads for the biodiesel test. However, it increases to 6.9 bar/deg for the same operating point at maximum AEC. The maximum PRR of ammonia/biodiesel is higher than pure biodiesel operation due to ignition delay and changing combustion mode from diffusion in pure biodiesel to the premixed combustion in dual-fuel mode, resulting in higher engine noise. However, the peak of PRR of ammonia biodiesel engine is lower than that of pure biodiesel at 20% of load. The flame propagation of ammonia/biodiesel in low loads is slower than the pure biodiesel due to the lean mixture, since the laminar flame speed of ammonia is slower in the lean mixture but faster in the stoichiometric condition.³⁹

MFB and HRR at 20% and 100% of the loads for ammonia/biodiesel along with biodiesel test are shown in Figure 7. HRR curves revealed that when more ammonia is injected into the intake manifold, the HRR peak increases. There are mainly two reasons: first, the higher amount of ammonia increases the peak of the in-cylinder pressure. Second, propagation of the premixed ammonia-air flame increases the HRR peak in the premixed

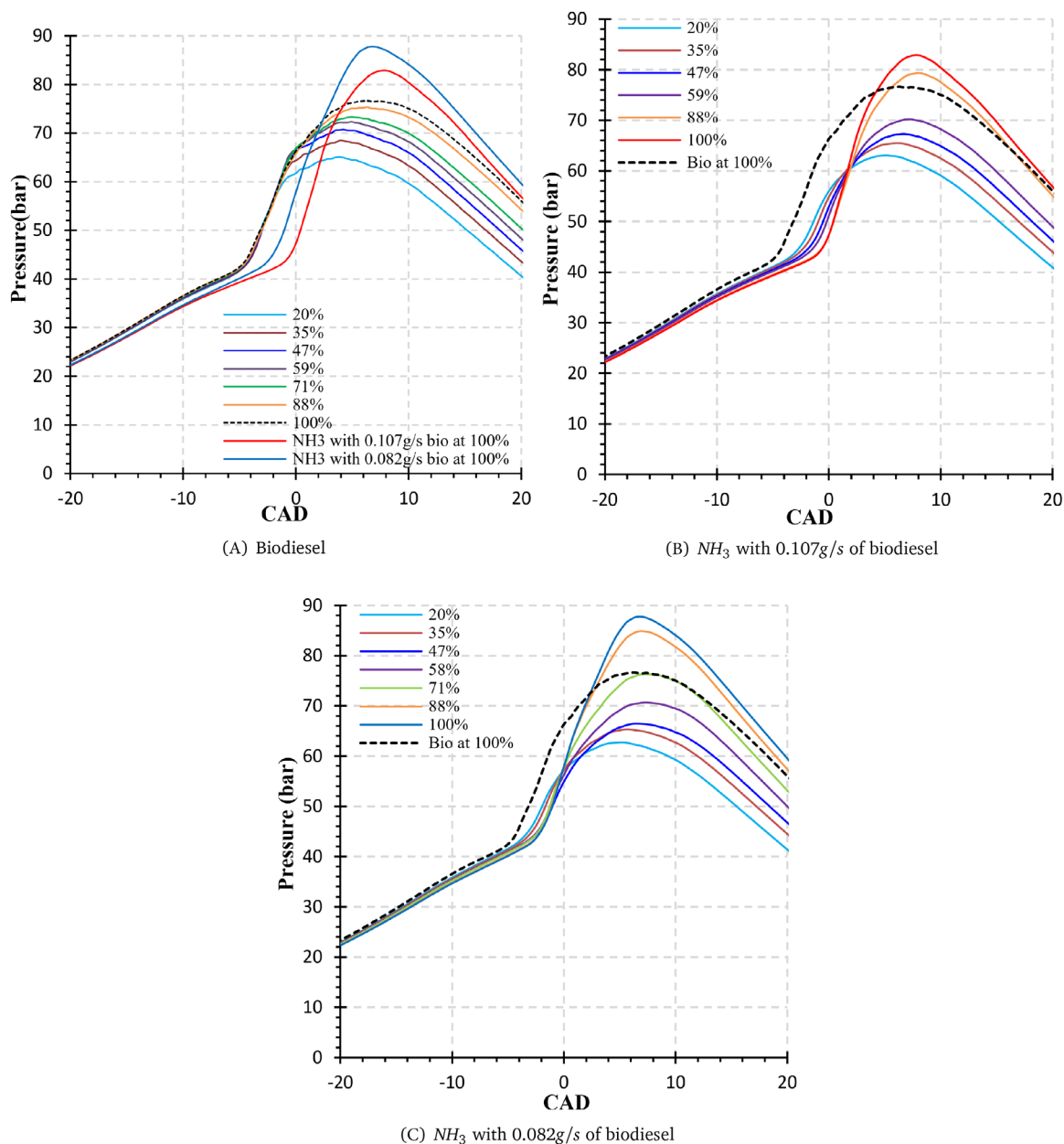


FIGURE 5 In-cylinder pressure profiles for each set of data

combustion phase in the HRR curve. Therefore, a higher ammonia ratio changed the combustion mode from diffusion mode to premixed combustion. Although pure biodiesel ignition starts in advance, the combustion of ammonia/biodiesel is finished earlier than only biodiesel for high loads, as can be observed in Figures 7B and 8C.

The indicators of ammonia with pilot biodiesel combustion are shown in Figure 8. SOC increases slightly from -5.83CAD to -5.24CAD by increasing the load for the pure biodiesel test. However, the minimum energy required to ignite the ammonia-air mixture is higher.⁴⁰ Therefore, biodiesel is first injected and then evaporated, providing energy to initiate the combustion of premixed ammonia-air. Therefore, ammonia with biodiesel in

dual-mode combustion has a longer delay in SOC, as can be observed in Figure 8A,B. SOC is delayed from -5.24CAD in pure biodiesel operation at full load to -1.43CAD and -2.55CAD for biodiesel/ammonia combustion in $\dot{m}_{\text{bio}} = 0.107\text{g/s}$ and $\dot{m}_{\text{bio}} = 0.082\text{g/s}$ tests, respectively, in the same operating point. Figure 8D shows the CA50-CA10 that is related to flame propagation. Thus, the flame propagation of ammonia/biodiesel in low loads is slower than that in the pure diesel case due to the lean mixture as well as the low flame speed of ammonia in lean condition. However, the ammonia flame propagates faster than pure biodiesel in higher loads because combustion mode is changed from the diffusion combustion in pure biodiesel to the premixed

combustion in dual-fuel mode. Moreover, the laminar flame speed of ammonia increases from the lean mixture to the stoichiometric condition.³⁹

CD is defined as the difference between CA90 and CA10. The CD of ammonia/biodiesel combustion has slightly increased for higher load, unlike biodiesel. However, the CD of biodiesel combustion increases as the load increases due to the high biodiesel mass flow rate and diffusion combustion. Therefore, premixed ammonia air burns earlier than pure biodiesel at high load as a result of the higher premixed ratio. Furthermore, the CA90 curve is presented in Figure 8E for set 1 and set

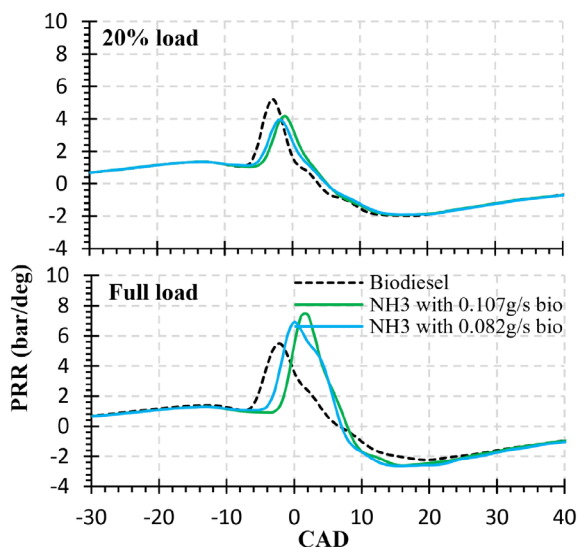


FIGURE 6 Pressure rise rate curves for loads of 20% and 100% in set 1, set 2, and biodiesel

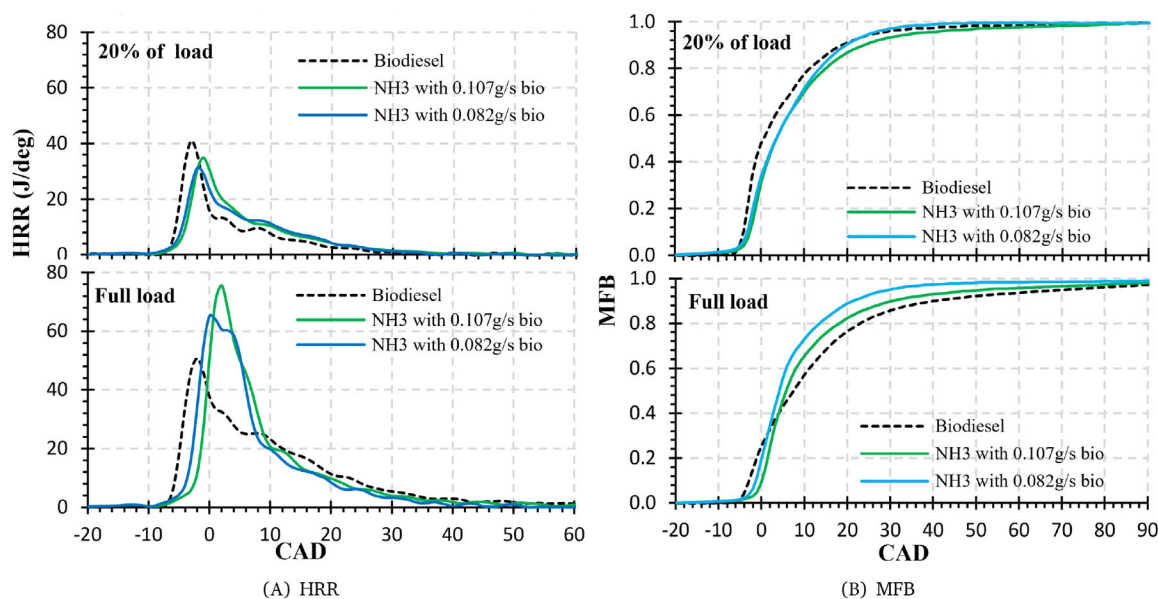


FIGURE 7 Mass fraction burned and heat release rate profiles for loads of 20% and 100% for each test (set 1, set 2, and biodiesel)

2 together with the biodiesel test. It can be observed that increasing the mass flow rate of pure biodiesel enhanced CA90, for example, 90% of pure biodiesel has been burned at 40.6CAD. It can be concluded that ammonia/biodiesel burns slower than only biodiesel at lower loads, but the CD of pure biodiesel is higher at high loads.

3.3 | Effects of ammonia on emissions

In this section, the influence of various ammonia mass flows with constant biodiesel flow ($\dot{m}_{bio} = 0.107\text{g/s}$ and $\dot{m}_{bio} = 0.082\text{g/s}$) will be discussed. The concentration of each species has been calculated in 5% O_2 to show the exhaust gas composition with the same level of dilution by air, and it should be noted that for each test the excess air was different. As more biodiesel is replaced by ammonia, it significantly reduces CO_2 , as shown in Figure 9. This can be expected since NH_3 has a carbon-free nature. The concentration of CO_2 in the biodiesel test is approximately 10.6% for different loads, however, it dramatically reduced to 2.48% for set 2 at full load, as can be observed in Figure 9B. Although CO_2 decreased significantly, it also produced N_2O around 60 ppm which has a global warming potential (GWP) of 298 times that of CO_2 over a 100-year timescale. Thus, 60 ppm of N_2O is equivalent to 1.7% of CO_2 in terms of GWP. Therefore, the CO_2 emission decreased from 10.6 to 4.26%, considering the equivalent GWP.

As discussed before, ammonia decreases the in-cylinder temperature. Hence, unsuccessful combustion at 20% of load due to low in-cylinder temperature causes a high amount of unreacted species such as NO , CO , and

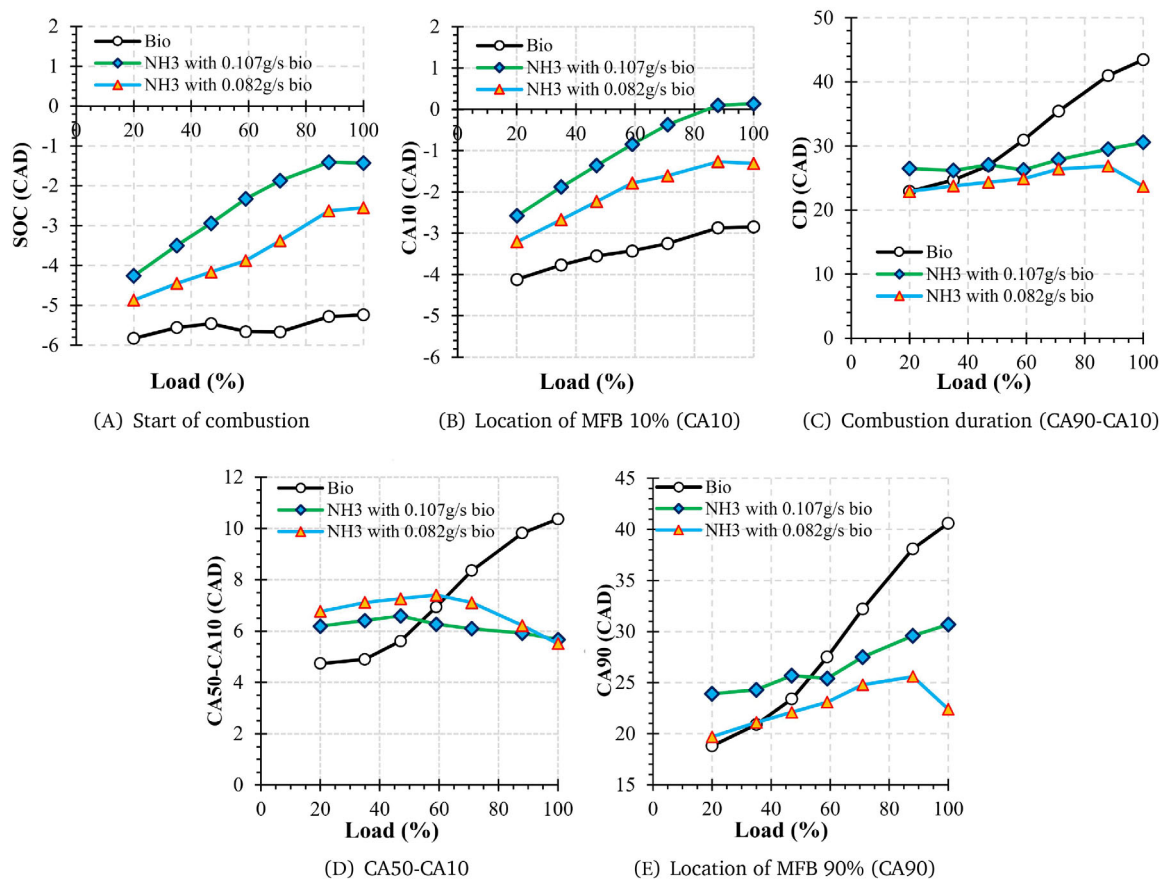


FIGURE 8 Ammonia/biodiesel and biodiesel combustion analysis indicators

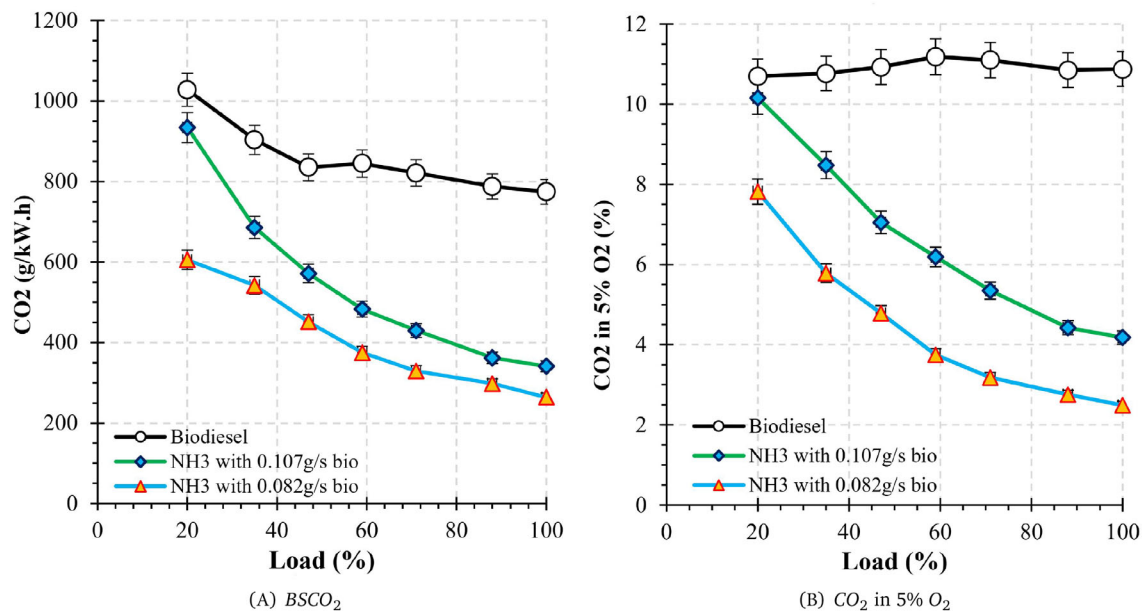


FIGURE 9 Comparison of CO₂ emissions between NH₃ with 0.107 g/s of bio and NH₃ with 0.082 g/s of bio with only biodiesel operation

PM (Figure 10B, 11B and 13). Observations of the NO emission in Figure 10 reveal that as more biodiesel is replaced by ammonia increases NO emission compared

with the only biodiesel test due to the presence of the N atom in NH₃. Furthermore, NO concentration curves for ammonia/biodiesel operation illustrate an interesting

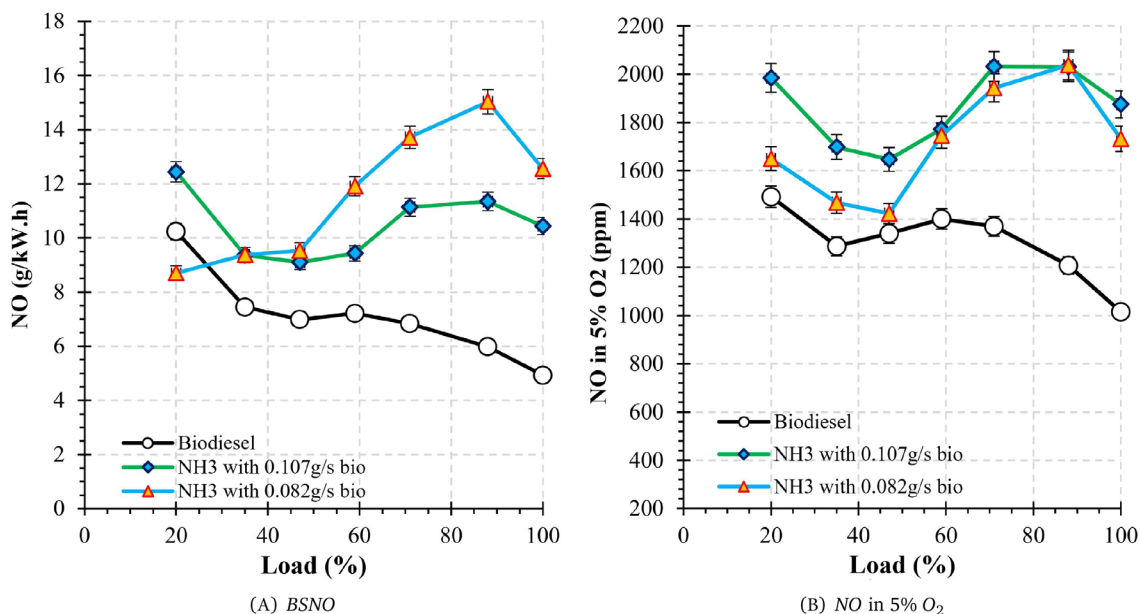


FIGURE 10 NO emissions of NH₃ with 0.107 g/s of bio and NH₃ with 0.082 g/s of bio compared with only biodiesel

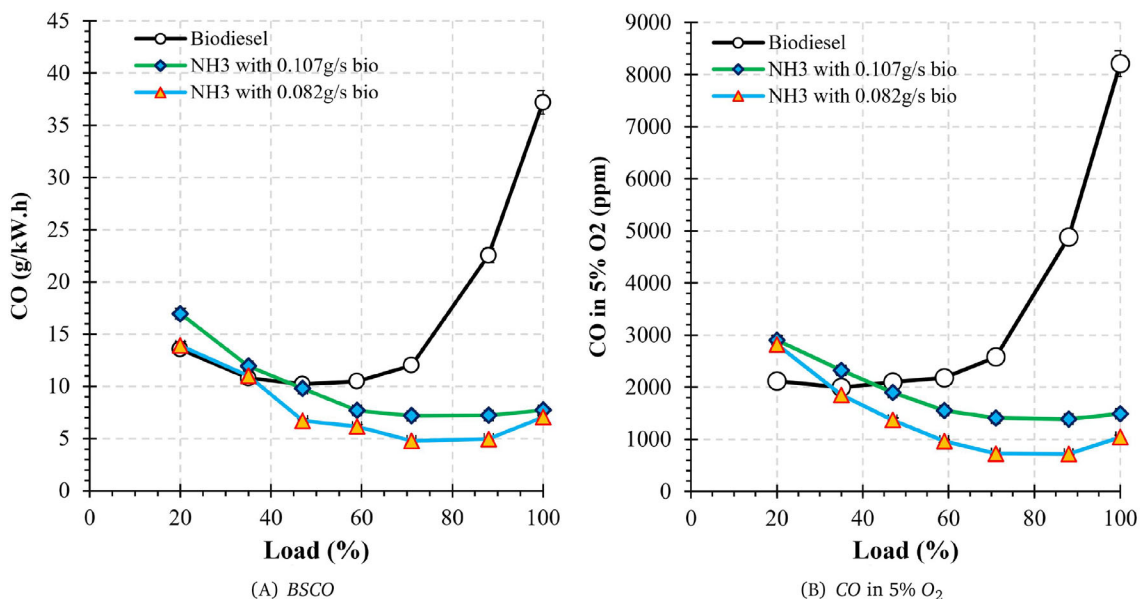


FIGURE 11 CO emissions of NH₃ with 0.107 g/s and with 0.082 g/s of biodiesel along with using only biodiesel

behavior, first decreasing until 50% of load, then increasing. This decrease of NO in 20% to 50% of the load is because of in-cylinder temperature, which results in destructing NO through reactions of 7 to 10. These reactions are started at temperature around 1100 K to 1400 K,^{41,42} where in-cylinder temperature is in the range of 20% to 50% of load for ammonia/biodiesel test.

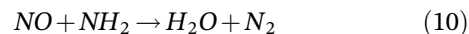
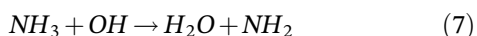


Figure 11 shows the CO emission for two sets of ammonia/biodiesel tests together with normal biodiesel

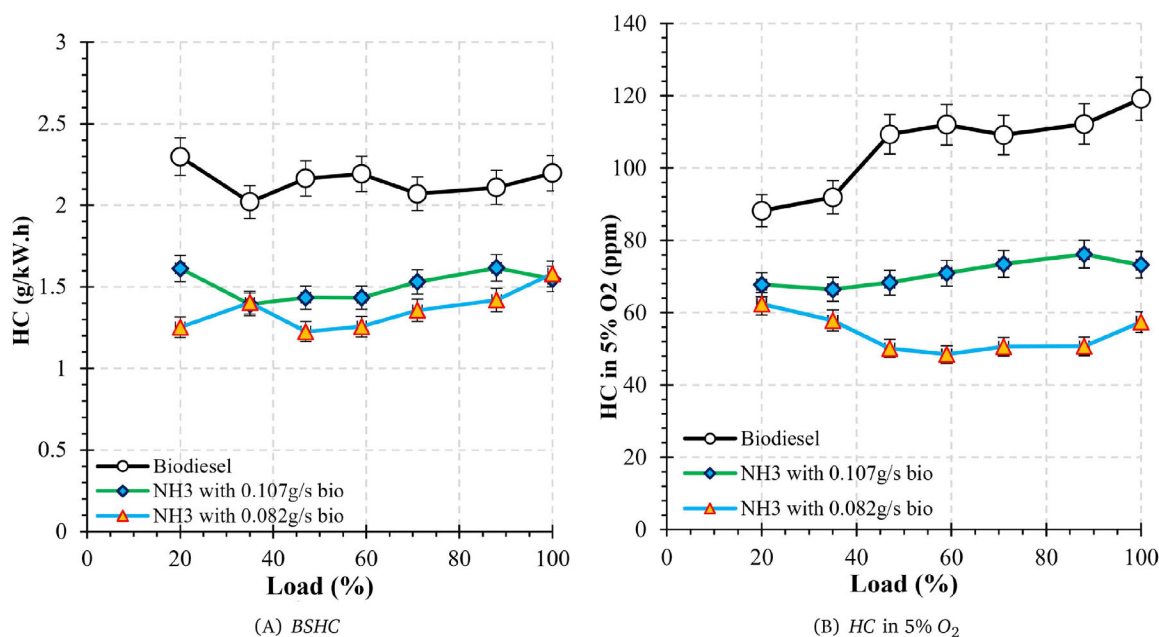


FIGURE 12 HC emissions of NH₃ with 0.107 g/s and 0.082 g/s of biodiesel compared with only biodiesel

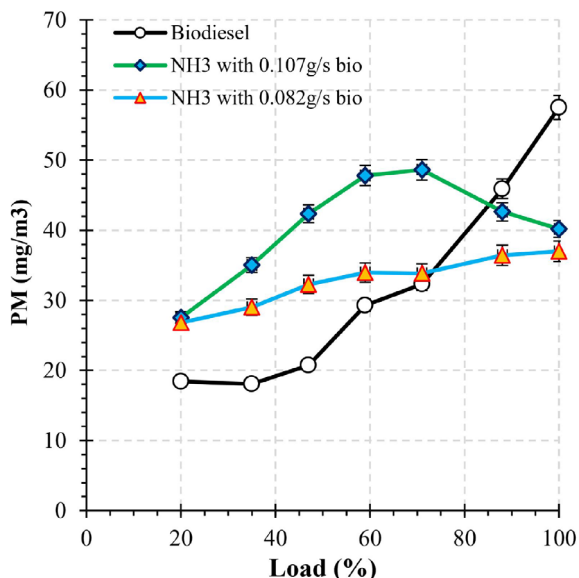


FIGURE 13 PM emission of test sets 1 and 2 compared with pure biodiesel

operation. Although the concentration of CO increases exponentially with increasing load due to the lack of O₂ at higher loads, it has decreased for the operation of ammonia/biodiesel. This decrease in CO is due to the low amount of carbon and premixed ammonia-air combustion. Therefore, the CO emission decreased significantly from 8210 ppm for biodiesel to 1042 ppm for set 2 at full load; in other words, the ammonia/biodiesel-fueled engine produces 35.18 g/kW.h less CO compared with the normal biodiesel engine, as shown in Figure 11B.

Figure 12A,B show HC emissions for ammonia/biodiesel engine including pure biodiesel at different loads. HC concentration slightly increases from 88 ppm to 199 ppm by enhancing the load. However, biodiesel generally produces a lower amount of HC emission in contrast to diesel fuel due to the content of O, resulting in complete combustion.⁴³⁻⁴⁵ Nevertheless, as more ammonia is introduced into the intake manifold, the emission of HC decreases. For example, the equivalent concentration of HC is reduced from 119 ppm for pure biodiesel to 73 and 57 for ammonia with $\dot{m}_{bio} = 0.107\text{g/s}$ and ammonia with $\dot{m}_{bio} = 0.082\text{g/s}$ test, respectively, in full load operation (Figure 12B). This decline could be due to a couple of reasons. First, due to homogeneous premixed ammonia-air combustion with a low amount of carbon. Second, since the biodiesel dose only contributes 10% and 3.5% of the load in the set 1 and set 2 tests, it is attesting that spraying a small dose of biodiesel will not impinge on the cylinder wall, the small size of the droplets and complete combustion in the thin clearance between the cylinder and piston. All of this results in a decrease in the HC emission.^{46,47}

Furthermore, PM emission for ammonia/biodiesel-fueled engine is presented in Figure 13. Typically, as the load increases, the formation of PM increases as a result of the high quantity of biodiesel fuel at high loads. Therefore, the higher the in-cylinder temperature, the longer the diffusion combustion phase, the constant SOI, and the decrease in the oxidation of the soot at high loads promote numerous PM formations. However, the ammonia/biodiesel-fueled engine has higher PM emission compared with the reference biodiesel in low loads.

PM increases slightly as the AEC increases. This has also been addressed by other researchers.^{37,48} As discussed in the previous section, enhancing ALC decreases CD and the in-cylinder temperature, which support the formation of PM. However, PM was lower in dual-fuel mode at full load compared with pure biodiesel operation. This is mainly due to the perfect mixing of biodiesel with pre-mixed ammonia-air since ammonia was injected to obtain higher loads instead of biodiesel.

4 | CONCLUSION

This study demonstrates utilizing ammonia as a potential carbon-free fuel with biodiesel in the CI engine in dual-fuel mode. An experimental study along with a 1D model has been conducted to investigate the impacts of different ammonia and biodiesel load contributions on ammonia/biodiesel combustion, engine performance, and emissions. Therefore, the engine runs first with two different pilot doses of biodiesel at low loads, then ammonia is injected into the intake port to obtain higher loads. The main conclusions drawn from this study are summarized as follows:

- Ammonia-/biodiesel-fueled engine has a lower BTE compared with pure biodiesel at the same operating point. Additionally, as more biodiesel was replaced by ammonia, BTE decreased as a result of unsuccessful combustion of ammonia/biodiesel. Therefore, the BTE decreased from 31.8 for pure biodiesel to 29.4 for the highest ammonia input energy ratio at full load.
- Increasing ammonia input energy contribution (AEC) decreases the exhaust gas temperature. Therefore, the exhaust gas temperature was reduced by 100 K when the AEC was 69.4%.
- Increasing ALC increases the peak of in-cylinder pressure, for example, in-cylinder pressure of ammonia/biodiesel combustion increased by 11.15 bar compared with biodiesel at full load because the SOC and peak of HRR diagram occur close to the TDC (0CAD). Moreover, ammonia also increases the peak of the pressure rise rate diagram.
- The SOC is delayed with increasing AEC; additionally, the propagation of the ammonia/biodiesel flame is slower than the only biodiesel mode in low load due to the low flame speed of ammonia in the lean mixture. The SOC was delayed by 2.6 CAD and CD was reduced by 19.7 CAD at maximum load compared with the same operating point with pure biodiesel.
- Ammonia increases the peak of the HRR and decreases the diffusion combustion phase in the HRR diagram. Therefore, as more ammonia is introduced

into the intake manifold, the combustion mode changes from diffusion to premixed combustion.

- As more biodiesel was replaced by ammonia, CO_2 , CO , and HC emissions decreased significantly. The minimum CO_2 , CO , and HC emissions were achieved when the AEC was the highest ($AEC = 69.4\%$). Therefore, CO_2 decreases by 510 g/kW.h and CO reduces by 30.1 g/kW.h at the maximum AEC. However, NO emission increased with increasing ammonia flow since NH_3 consists of one nitrogen atom.

NOMENCLATURE

ABDC	after bottom dead center
AEC	ammonia energy contribution
ALC	ammonia load contribution
ATDC	after top dead center
BBDC	before bottom dead center
BDC	bottom dead center
BLC	biodiesel load contribution
BSFC	brake-specific fuel consumption
BTDC	before top dead center
BTE	brake thermal efficiency
CA10	CAD value for 10% MFB
CA50	CAD value for 50% MFB
CA90	CAD value for 90% MFB
CAD	crank angle degree
CD	combustion duration
CI	compression ignition
CR	compression ratio
EVC	inlet valve closing
EVO	exhaust valve opening
GDI	gasoline direct injection
GWP	global warming potential
HRR	heat release rate
ICE	internal combustion engine
IVC	inlet valve closing
IVO	inlet valve opening
LHV	lower heating value
MFB	mass fraction burned
P_b	brake power
rpm	rotation per minute
SCR	selective catalytic reduction
SI	spark ignition
SOC	start of combustion
SOI	start of injection
TDC	top dead center
w_{NH_3}	NH_3 ratio in fuel

AUTHOR CONTRIBUTION

Ebrahim Nadimi: Conceptualization, Methodology, Software, Validation, Formal analysis, Investigation, Experiment,

Data Curation, Figures, Original draft, Writing—Review and editing. **Grzegorz Przybyła**: Conceptualization, Methodology, Investigation, Experiment, Supervision, Writing—review and editing. **David Robert Emberson**: Writing—review and editing. **Terese Løvås**: Writing—review and editing. **Łukasz Ziółkowski**: Experiment. **Wojciech Adamczyk**: Writing—review and editing, project administration.

ACKNOWLEDGEMENT

The authors also thank AVL List GmbH for providing the license according to the university and AVL agreement.

FUNDING INFORMATION

This work was financed by Norway and Poland grants (Contract NO. NOR/POLNOR/ACTIVATE/0046/2019-00) to ACTIVATE project “Ammonia as carbon free fuel for internal combustion engine driven agricultural vehicle” (<https://ammoniaengine.org>.)

CONFLICT OF INTEREST

The authors have no conflict of interest to report.

ORCID

Ebrahim Nadimi  <https://orcid.org/0000-0003-3338-5288>

Grzegorz Przybyła  <https://orcid.org/0000-0001-8089-3475>

Wojciech Adamczyk  <https://orcid.org/0000-0002-9178-9566>

REFERENCES

- Liobikienė G, Butkus M. The European Union possibilities to achieve targets of Europe 2020 and Paris agreement climate policy. *Renew Energy*. 2017;106:298-309.
- Venugopal T, Sharma A, Satapathy S, Ramesh A, Gajendra Babu M. Experimental study of hydrous ethanol gasoline blend (e10) in a four stroke port fuel-injected spark ignition engine. *Int J Energy Res*. 2013;37(6):638-644.
- Sun C, Liu Y, Qiao X, et al. Experimental study of effects of exhaust gas recirculation and combustion mode on combustion, emission, and performance of DME-methanol-fueled turbocharged common-rail engine. *Int J Energy Res*. 2022;46(3):2385-2402.
- Venkanna B, Venkataramana Reddy C. Direct injection diesel engine performance, emission, and combustion characteristics using diesel fuel, nonedible honne oil methyl ester, and blends with diesel fuel. *Int J Energy Res*. 2012;36(13):1247-1261.
- Valera-Medina A, Xiao H, Owen-Jones M, David WI, Bowen P. Ammonia for power. *Progr Energy Combust Sci*. 2018;69:63-102.
- Valera-Medina A, Amer-Hatem F, Azad A, et al. Review on ammonia as a potential fuel: from synthesis to economics. *Energy Fuel*. 2021;35(9):6964-7029.
- Wijayanta AT, Oda T, Purnomo CW, Kashiwagi T, Aziz M. Liquid hydrogen, methylcyclohexane, and ammonia as potential hydrogen storage: comparison review. *Int J Hydrogen Energy*. 2019;44(29):15026-15044.
- Frigo S, Gentili R. Analysis of the behaviour of a 4-stroke si engine fuelled with ammonia and hydrogen. *Int J Hydrogen Energy*. 2013;38(3):1607-1615.
- MacKenzie J. J., Avery W. H., Ammonia fuel: the key to hydrogen-based transportation. Technical Report. Inst of Electrical and Electronics Engineers, Piscataway, NJ (United States). 1996.
- Lhuillier C, Brequigny P, Contino F, Mounaïm-Rousselle C. Experimental investigation on ammonia combustion behavior in a spark-ignition engine by means of laminar and turbulent expanding flames. *Proc Combust Inst*. 2021;38(4):5859-5868.
- Koch E. Ammonia—a fuel for motor buses. *J Inst Pet*. 1945;31:213.
- Starkman ES, Newhall H, Sutton R, Maguire T, Farbar L. Ammonia as a spark ignition engine fuel: theory and application. *SAE Trans*. 1967;75:765-784.
- Starkman ES, James G, Newhall H. Ammonia as a diesel engine fuel: theory and application. *SAE Trans*. 1968;76:3193-3212.
- Pearsall TJ, Garabedian CG. Combustion of anhydrous ammonia in diesel engines. *SAE Transactions*. 1968;76:3213-3221.
- Sawyer R. F., Starkman E. S., Muzio L., Schmidt W., Oxides of Nitrogen in the Combustion Products of an Ammonia Fueled Reciprocating Engine, Technical Report, SAE Technical Paper. 1968.
- Mounaïm-Rousselle C, Brequigny P. Ammonia as fuel for low-carbon spark-ignition engines of tomorrow's passenger cars. *Frontiers Mech Eng*. 2020;6:70.
- Schönborn A., Aqueous solution of ammonia as marine fuel, Proceedings of the Institution of Mechanical Engineers, Part M: Journal of Engineering for the Maritime Environment 2021; 235(1):142-151.
- Grannell SM, Assanis DN, Bohac SV, Gillespie DE. The fuel mix limits and efficiency of a stoichiometric, ammonia, and gasoline dual fueled spark ignition engine. *J Eng Gas Turb Power*. 2008;130(4).
- Salek F, Babaie M, Shakeri A, Hosseini SV, Bodisco T, Zare A. Numerical study of engine performance and emissions for port injection of ammonia into a gasoline-ethanol dual-fuel spark ignition engine. *Applied Sciences*. 2021;11(4):1441.
- Yapicioglu A, Dincer I. Experimental investigation and evaluation of using ammonia and gasoline fuel blends for power generators. *Appl Therm Eng*. 2019;154:1-8.
- Mounaïm-Rousselle C, Bréquigny P, Dumand C, Houillé S. Operating limits for ammonia fuel spark-ignition engine. *Energies*. 2021;14(14):4141.
- Lhuillier C, Brequigny P, Contino F, Mounaïm-Rousselle C. Experimental study on ammonia/hydrogen/air combustion in spark ignition engine conditions. *Fuel*. 2020;269:117448.
- Oh S, Park C, Kim S, Kim Y, Choi Y, Kim C. Natural gas-ammonia dual-fuel combustion in spark-ignited engine with various air-fuel ratios and split ratios of ammonia under part load condition. *Fuel*. 2021;290:120095.
- Dimitriou P, Javaid R. A review of ammonia as a compression ignition engine fuel. *Int J Hydrogen Energy*. 2020;45(11):7098-7118.
- Reiter AJ, Kong S-C. Combustion and emissions characteristics of compression-ignition engine using dual ammonia-diesel fuel. *Fuel*. 2011;90(1):87-97.

26. Reiter AJ, Kong S-C. Demonstration of compression-ignition engine combustion using ammonia in reducing greenhouse gas emissions. *Energy Fuel*. 2008;22(5):2963-2971.
27. Lee D, Song HH. Development of combustion strategy for the internal combustion engine fueled by ammonia and its operating characteristics. *Journal of Mechanical Science and Technology*. 2018;32(4):1905-1925.
28. Yousefi A, Guo H, Dev S, Liko B, Lafrance S. Effects of ammonia energy fraction and diesel injection timing on combustion and emissions of an ammonia/diesel dual-fuel engine. *Fuel*. 2021;134:122723.
29. Boost A., 2-theory, AVL List GmbH 769.
30. Kobayashi H, Hayakawa A, Somarathne KKA, Okafor EC. Science and technology of ammonia combustion. *Proc Combust Inst*. 2019;37(1):109-133.
31. Lewandowski DA. *Design of Thermal Oxidation Systems for Volatile Organic Compounds*. CRC Press; 2017.
32. Salek F, Babaie M, Redel-Macias MD, et al. The effects of port water injection on spark ignition engine performance and emissions fueled by pure gasoline, e5 and e10. *Processes*. 2020;8(10):1214.
33. Hasan AO, Al-Rawashdeh H, Ala'a H, Abu-Jrai A, Ahmad R, Zeaiter J. Impact of changing combustion chamber geometry on emissions, and combustion characteristics of a single cylinder si (spark ignition) engine fueled with ethanol/gasoline blends. *Fuel*. 2018;231:197-203.
34. Hasan AO, Osman AI, Ala'a H, et al. An experimental study of engine characteristics and tailpipe emissions from modern diesel engine fuelled with methanol/diesel blends. *Fuel Process Technol*. 2021;220:106901.
35. Gross CW, Kong S-C. Performance characteristics of a compression-ignition engine using direct-injection ammonia-dme mixtures. *Fuel*. 2013;103:1069-1079.
36. Kuta K., Nadimi E., Przybyła G., Żmudka Z., Adamczyk W., Ammonia Ci Engine Aftertreatment Systems Design and Flow Simulation
37. Frost J, Tall A, Sheriff AM, Schönborn A, Hellier P. An experimental and modelling study of dual fuel aqueous ammonia and diesel combustion in a single cylinder compression ignition engine. *Int J Hydrogen Energy*. 2021;46(71):35495-35510.
38. Heywood J., Internal combustion engine fundamentals mcgraw-hill book co, New York
39. Ichimura R, Hadi K, Hashimoto N, Hayakawa A, Kobayashi H, Fujita O. Extinction limits of an ammonia/air flame propagating in a turbulent field. *Fuel*. 2019;246:178-186.
40. Pfahl U, Ross M, Shepherd J, Pasamehmetoglu K, Unal C. Flammability limits, ignition energy, and flame speeds in h₂-ch₄-nh₃-n₂-o₂-n₂ mixtures. *Combust Flame*. 2000;123(1-2):140-158.
41. Lyon RK. The nh₃-no-o₂ reaction. *Int J Chem Kinet*. 1976;8(2): 315-318.
42. Lee G-W, Shon B-H, Yoo J-G, Jung J-H, Oh K-J. The influence of mixing between nh₃ and no for a de-nox reaction in the SNCR process. *J Ind Eng Chem*. 2008;14(4):457-467.
43. Shirneshan A. Hc, co, co₂ and nox emission evaluation of a diesel engine fueled with waste frying oil methyl ester. *Procedia Soc Behav Sci*. 2013;75:292-297.
44. Payri F, Bermúdez VR, Tormos B, Linares WG. Hydrocarbon emissions speciation in diesel and biodiesel exhausts. *Atmos Environ*. 2009;43(6):1273-1279.
45. Raja KSS, Srinivasan SK, Yoganandam K, Ravi M. Emissions and performance investigation on the effect of dual fuel injection in biodiesel driven diesel engine. *Energy Sourc A Recov Utilizat Env Effects*. 2021;1-11.
46. Matsui Y., Sugihara K., Sources of Hydrocarbon Emissions from a Small Direct Injection Diesel Engine, Technical Report, SAE Technical Paper. 1987.
47. Khair M. K., Jääskeläinen H., Emission Formation in Diesel Engines. 2008.
48. Kane SP, Northrop WF. Thermochemical recuperation to enable efficient ammonia-diesel dual-fuel combustion in a compression ignition engine. *Energies*. 2021;14(22):7540.

How to cite this article: Nadimi E, Przybyła G, Emberson D, Løvås T, Ziółkowski Ł, Adamczyk W. Effects of using ammonia as a primary fuel on engine performance and emissions in an ammonia/biodiesel dual-fuel CI engine. *Int J Energy Res*. 2022;46(11):15347-15361. doi:10.1002/er.8235